1.5

IMPROVING THE SPECIFICATION OF SUB-GRID OROGRAPHY IN NWP DRAG PARAMETRIZATIONS.

Stuart Webster*Met Office, Exeter, Devon, U.K.

1. INTRODUCTION

The current Unified Model (UM) sub-grid scale orographic (SSO) drag parametrization (Webster *et al.*, 2003) has been used in the Met Office operational global forecast model since August 2002. The implementation of this scheme led to significant improvements in forecast skill, especially at low levels where the drag due to the flow blocking component of the scheme was particularly beneficial. In addition to these improvements in skill, an important feature of the current scheme is that it is relatively simple and therefore it provides a sound basis for future developments.

In this paper, two such developments that were implemented into the global forecast model in April 2004 are described and illustrated. The first change is to use a higher resolution source orography dataset and, more precisely, to ensure that the anisotropy of the SSO is calculated in a much more robust way. This change has led to the implementation of the scheme *without retuning* in the operational 20km European model (EuroLAM) and 12km (UK mesoscale) limited area forecast models. Previously the scheme was not implemented in the EuroLAM and was implemented with significant retuning in the UK mesoscale model. The second change is to increase the component of the total surface stress attributed to flow blocking. As we shall show, the associated reduction in the stratospheric gravity-wave drag leads to large improvements in stratospheric wind errors in the global forecast model.

In section 2, the key features of the current scheme associated with the two recent developments are briefly described. In section 3, the calculation of the SSO anisotropy fields and the associated improvement to the calculation is described. In section 4, the rationale behind attributing more of the total drag to flow-blocking is discussed and the impact of this change illustrated. Finally, in section 5 the current status of the SSO parametrization is summarised and potential future developments discussed.

* Corresponding author address: Stuart Webster, Met Office, Exeter, Devon, EX1 3PB, U.K.; email:stuart.webster@metoffice.com

2. OUTLINE OF THE CURRENT SCHEME

The current scheme is very simple and thus uses the analytic expression for linear two-dimensional non-rotating frictionless flow as its prediction of the surface stress as follows

$$\tau_{sx} = \rho U N \hat{K}^{-1}(\sigma_{xx}\cos\chi + \sigma_{xy}\sin\chi) \quad (1)$$

$$\tau_{sy} = \rho U N \hat{K}^{-1}(\sigma_{xy}\cos\chi + \sigma_{yy}\sin\chi) \quad (2)$$

where τ_{sx} and τ_{sy} are the zonal and meridional components of the surface stress respectively, ρ is the low-level density, U is the low-level wind speed, N is the low-level buoyancy frequency, χ is the direction of the low-level wind relative to westerly, $\hat{K}$ is a "tuneable" wavenumber constant, and the σ_{ij} are the squared grid-box-average gradients (the variance of the gradients) of the source dataset. These gradient terms replace the variance, σ^2, used in the original gravity wave drag schemes such as described in Palmer *et al.* (1986) and are what describe the anisotropy of the SSO. The modification to the way in which they are calculated is the focus of section 3.

The surface stress is then partitioned into blocked flow and gravity wave drag components depending on the low level Froude number, F_r. Specifically, the depth of the layer of air flowing over the SSO is diagnosed as

$$t = \frac{U_\tau}{F_{rc} N} \quad (3)$$

where U_τ is the component of the wind $\mathbf{U} = (u, v)$ in the direction of the surface stress vector $\tau_\mathbf{s} = (\tau_{sx}, \tau_{sy})$ and F_{rc} is the F_r at which flow blocking is deemed to first occur. This is the second "tuneable" parameter within the scheme, and the recent retuning of this parameter is the focus of section 4. The gravity wave component of the surface stress is then evaluated as

$$\tau_{\mathbf{gwd}} = \tau_\mathbf{s} \cdot \left(\frac{t}{h}\right)^2. \quad (4)$$

where h is the height of the SSO, and is taken to be 2.5σ above the resolved orography. The gravity wave stress is then carried upwards from the height h and

deposited according to a wave saturation hypothesis, whilst the flow blocking stress is deposited linearly with height from the surface up to the height, h.

3. THE CALCULATION OF THE SSO ANISOTROPY

3.1 The robustness problem of the SSO statistics

As already discussed above, the anisotropy of the SSO is input into the parametrization via the σ_{ij} terms. As described in Gregory *et al.* (1998), these terms derive from considering the spectral properties of the source orography within a model gridbox. The functional form of the spectrum of the orographic variances is chosen so that the anisotropy of the orography can be accounted for, since it is the component of the wind perpendicular to a ridge that generates the drag we wish to parametrize. However, although representing the anisotropy is beneficial, a problem with the σ_{ij} terms is that they do not converge as higher and higher resolution datasets are used, i.e. their amplitudes continue to increase as more and more scales are included in their calculation. As illustrated by Taylor *et al.* (1997), this appears to be a problem with any higher order property of the SSO used to describe the anisotropy of the SSO, i.e. the problem is not peculiar to the SSO statistics used in the UM. The lack of convergence of the higher order properties is in contrast to the mean and variance fields which do converge with increasing data resolution.

To illustrate this point, consider an orographic profile, h_k, consisting of a single Fourier mode with amplitude h_0 and wavenumber, k. Then

$$h_k = h_0 \cos kx \tag{5}$$

and the variance of this profile (averaged over a wavelength) is,

$$\sigma^2 = h_0^2/2, \tag{6}$$

whilst the variance of the gradient is

$$\sigma_{xx} = k^2 h_0^2/2. \tag{7}$$

The surface stress based on the original variance based equation (e.g. as used in Palmer *et al.*, 1986) is

$$\tau_{sx} = \rho U N k \sigma^2 \tag{8}$$

whilst that based on the variance of the gradients is given by

$$\tau_{sx} = \rho U N \sigma_{xx}/k. \tag{9}$$

In this simple case, the surface stress is the same using either approach.

Now consider the realistic case where the orographic profile is the sum over many discrete wavenumbers (though still only considering variations in x). Then

$$\sigma^2 = \sum_{k=k_l}^{k=ku} h_0(k)^2/2 \tag{10}$$

and

$$\sigma_{xx} = \sum_{k=k_l}^{k=ku} k^2 h_0(k)^2/2, \tag{11}$$

where k_u is the highest wavenumber (corresponding to the resolution of the dataset), and k_l is the lowest wavenumber (corresponding to the highest wavenumber not resolved by the model) in the orographic profile. In both cases, a single typical wavenumber, $\hat{K}$ (as defined for Eqs. (1) and (2)), is used when calculating the surface stress. Thus, the calculation of the surface stress based on σ^2 becomes

$$\tau_{sx} = \rho U N \hat{K} \sum_{k=k_l}^{k=ku} h_0(k)^2/2, \tag{12}$$

whilst the calculation based on σ_{xx} is the one-dimensional version of Eq. (1) and becomes

$$\tau_{sx} = \frac{\rho U N}{\hat{K}} \sum_{k=k_l}^{k=ku} k^2 h_0(k)^2/2. \tag{13}$$

These drag predictions will only converge if σ^2 and σ_{xx} converge when higher and higher wavenumbers are included in the source dataset.

The typical properties of Eqs. (10) and (11) is illustrated in Fig. 1, which shows their power spectra over an area of the European Alps. The x-axis in all the plots is the wavenumber, k, with for example, $k = 1$ corresponding to a wavelength of about 6km. Figure 1(a) shows the variance (σ^2) spectra whilst Fig. 1(b) shows the variance of the gradient (σ_{xx}) spectra plotted on a log-log scale. For the unfiltered source dataset (thick solid line), the power in the σ^2 spectra diminishes with a slope of about -1.3 for $0.1 < k < 1$, which is broadly consistent with the findings of many previous studies (see Uhrner (2001) for some recent calculations). In contrast, the power in the σ_{xx} spectra is much more uniform.

The impact of the differing shapes of the σ^2 and σ_{xx} spectra on their convergence properties is seen most clearly by replotting the spectra on a linear scale, since then the amplitude of the fields are proportional to the area under the power spectra curves.

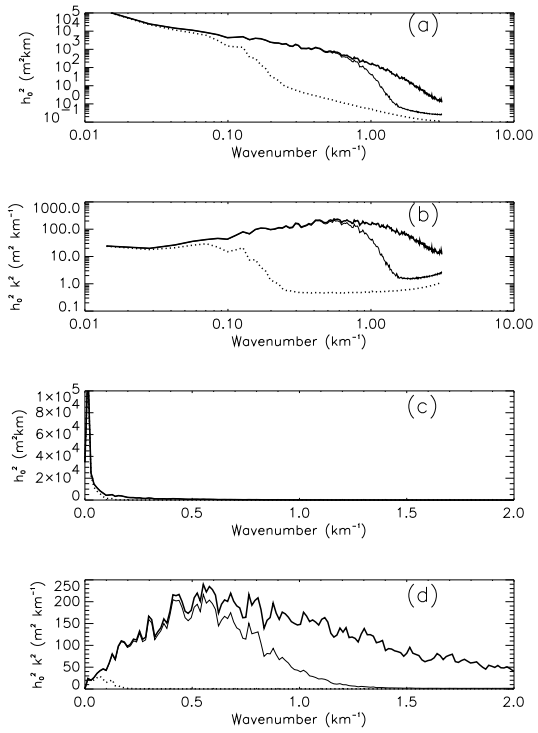

Figure 1: (a) One dimensional variance (σ^2) spectra for a 400km×400km region over the European Alps. The spectra are computed in the East-West direction and are the North-South average over all such sections within the domain. The thick solid line shows the spectra for the unfiltered data, the thin solid line shows the spectra for the proposed ($k_u = 1$) filtering and the thick dashed line shows the spectra for the currently implemented ($k_u = 0.2$) filtering. (b), as (a), but for the variance of the gradient (σ_{xx}) spectra. (c) and (d) show the same information as (a) and (b), but are plotted on a linear scale to more clearly illustrate the relative importance of the different wavenumbers in the respective calculations.

Thus, Fig 1(c) shows that most of the power in the σ^2 spectra is in the lowest wavenumber contributions ($k < 0.2$ corresponding to wavelengths greater than 30km) which is why the σ^2 calculation converges rapidly. In contrast, Fig. 1(d) shows that most of the power in the σ_{xx} spectra is in the high wavenumbers, with the maximum power at $k \approx 0.5$ (a wavelength of about 10km). This plot therefore provides a clear indication of why the σ_{xx} calculation does not converge when higher wavenumbers are included, and hence why the drag predicted by Eqs.(1) and (2) is not robust.

At the Met Office, the true extent of this convergence problem with the σ_{ij} calculations first became obvious when the the SSO parametrization was implemented in the UK mesoscale forecast model. The orography fields for this model are created from the DTED source dataset at 2km resolution (thus, with the mean orography filtering that is applied $k_l \approx 0.1$, whilst $k_u \approx 1.5$). This source dataset was thus at a much higher resolution than that used to calculate the mean orography and SSO fields for the (~ 60km) global forecast model which, at that time, were created from a 10' (~ 20km) resolution version of the GLOBE dataset (and thus $k_l \approx 0.025$ and $k_u \approx 0.15$). It is clear from Fig. 1(d) that the change in k_u will dominate the change in k_l when calculating the σ_{ij} terms. In fact, these fields turn out to be almost two orders of magnitude larger for the mesoscale model than for the global forecast model.

As a result of this difference in the σ_{ij} amplitudes the initial implementation of the SSO scheme in the UK mesoscale model used a value of $\hat{K}$ that was retuned to be 100 times larger than that used in the global forecast model, so that in Eqs. (1) and (2), the $\sigma_{ij}/\hat{K}$ amplitude, and hence the SSO drag amplitude was broadly similar in both models. With this retuning, the inclusion of the SSO scheme was found to improve the mesoscale model forecast skill. However, there is clearly no guarantee that the total (resolved plus parametrized) drag will be in any way similar in the two models. This is clearly undesirable and so the next section discusses the steps taken so far towards improving the robustness of the SSO statistics.

3.2 A more robust SSO specification

Ideally, the method of computing the σ_{ij} terms should minimise the need to retune the scheme when either the source dataset (and hence k_u) or the model resolution (and hence k_l) is changed. As already discussed, by far the largest sensitivity is to k_u and thus the modification to the calculation simply involves

specifying the value of k_u and then filtering higher wavenumbers from the source dataset. This clearly requires using high resolution datasets, and is now possible with global orography datasets available at 1km resolution (e.g. GLOBE). With k_u fixed in this way, the σ_{ij} fields will reduce to zero as the model resolution (k_l) increases to k_u. In this way, the total (resolved plus parametrized) drag for each model resolution should be similar to the high-resolution "truth" simulation, where $k_l = k_u$ and so all the drag is resolved.

One plausible choice for k_u is to consider only those scales which can generate gravity waves, i.e. consider only those scales at which N is important. For typical values of U and N, this suggests a $k_u \approx 1$. The scales for which $k > k_u$ should be represented by the turbulent form drag parametrization. The impact of removing the $k > 1$ scales from the Alps power spectra is shown in Fig. 1 by the thin solid line. This filtering is very scale selective, and thus has only a very small impact on the variance but will have a significant impact on the σ_{ij} fields, especially at higher model resolutions.

The actual choice of k_u implemented in April 2004 was rather more pragmatic, and ensured that $\hat{K}$ did not need retuning in the global forecast model where the scheme is already well tested. With this choice of k_u and the σ_{ij} fields computed from the 1' version of the GLOBE datset, the SSO scheme has been implemented in the global forecast model, the Euro-LAM and the UK mesoscale forecast models without retuning $\hat{K}$, and with neutral or positive impacts on forecast skill in each case.

However, as the thick dashed lines in Fig. 1 indicate, a large amount of filtering is necessary to keep $\hat{K}$ constant, and as a result features with $k > 0.2$ (wavelengths shorter than 30km) are eliminated from the source dataset. Note especially the size of the impact in Fig 1(d), which illustrates just how much the σ_{xx} calculation using the 1' dataset must be reduced to make it comparable to that using the 10' dataset. Thus, the current choice of filtering means that once the model resolution reaches about 7km (and so 30km features are well resolved) all the scales producing drag will be resolved and thus any further increase in resolution will not result in a further increase in drag. This is clearly at odds with the work of Smith *et al.* (paper 1.4, these proceedings) who in Mesoscale Alpine Programme (MAP) case studies have shown the resolved drag continuing to increase as the resolution is increased to 4km.

Thus, the current filtering is clearly excessive, but has allowed the SSO scheme to be implemented in all the current forecast models without retuning. In the future, the Smith *et al.* framework will be extended to investigate the total (resolved plus parametrized) drag and so will provide a test-bed for refining the filtering of the source data or, more generally, refining the definition of the SSO characteristics.

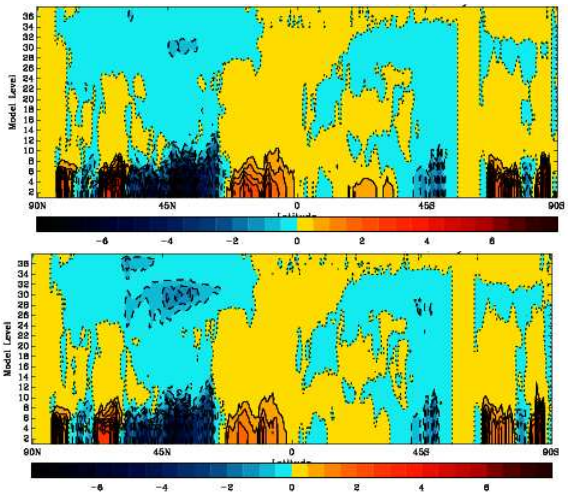

Figure 2: The forecast day 1 SSO zonal-mean zonal wind acceleration for the $F_{rc} = 4$ trial (top panel) and for the $F_{rc} = 2$ trial (bottom panel). These fields are the average of 31 forecasts in a pair of December global forecast trials. Contour interval is 0.5ms^{-1}d^{-1}.

4. Retuning of F_{rc}

The second development to be implemented in the global forecast model in April 2004 was a retuning of F_{rc}, which as seen from Eqs.(3) and (4), modifies the partitioning of the drag between the flow-blocking and gravity-wave components of the SSO scheme. The retuning was motivated by an increase in stratospheric wind errors associated with an increase in stratospheric gravity wave drag which only became obvious once the current scheme had become operational. The scheme can be expected to reduce these errors by increasing F_{rc}. Initial tests suggested increasing F_{rc} from 2 to 4 would significantly reduce these errors. However, it should be borne in mind that this obviously takes the value of F_{rc} further away from unity, which is the value consistent with the "cut off mountain" definition of the amplitude of the gravity waves, and so perhaps suggests that we are retuning F_{rc} to compensate for some other weakness in the scheme.

The impact of this change on the SSO drag in the

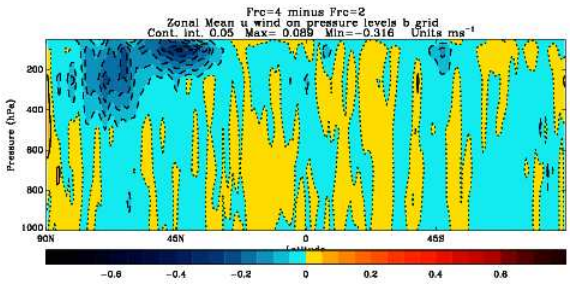

Figure 3: The difference in the average day 1 zonal-mean zonal wind root-mean-square (rms) error between the $F_{rc} = 4$ and $F_{rc} = 2$ trials.

global forecast model is illustrated in Fig. 2. The change in F_{rc} is most obvious at higher model levels (in the lower stratosphere) where the expected reduction in gravity wave drag for the $F_{rc} = 4$ trial is apparent. In both trials the low level flow-blocking drag is clearly much larger than the gravity wave drag. In fact, the $F_{rc} = 4$ trial attributes more than 95% of the total drag to flow blocking, which is clearly very different from the original orographic drag schemes which attributed all their drag to gravity waves.

The impact of this change on forecast performance is shown in Fig. 3, which shows the average zonal mean root-mean-square (rms) zonal wind errors at forecast day 1. The reduction in error at upper levels, i.e. at the same levels as where the GWD has been reduced, is very apparent and latitude-longitude sections at 100hPa (not shown) confirm that the improvements are over and downstream of the orography. At this level in fact, the improvement in the Northern Hemisphere rms wind errors is about 10% and even down at the 250hPa level an improvement of 1% is observed.

Thus, the simplicity of the SSO scheme has allowed us to affect a significant improvement in forecast skill by changing one of the two "tuneable" parameters in a predictable way.

5. SUMMARY

The current SSO scheme has been designed to be both simple and numerically robust when implemented into a model at a particular resolution. In this paper, we have extended the robustness issues to include the specification of the SSO characteristics. The work described here allows the same source orography to be used to calculate the resolved and SSO fields for any model resolution. Thus, as the model resolution increases, the parametrized scales are smoothly handed over to the resolved scales, and retuning the SSO scheme at each resolution should no longer be necessary.

The second change described retuned the partitioning of the flow-blocking and gravity-wave drag to address systematic stratospheric wind errors identified in the global forecast model.

The above changes were implemented into the global, EuroLAM and the UK mesoscale model in April 2004. Thus the orographic representation is now the same in all versions of the UM, with the same settings of $\hat{K}$ and F_{rc} used in all models. This should therefore allow future developments to the scheme to be implemented quickly into all versions of the UM.

In the future, the SSO characterisation and scheme behaviour will be further developed by using the MAP case study framework to assess the convergence properties of the current implementation and, hopefully, reduce the filtering so that the total drag converges to the correct high resolution "truth".

6. ACKNOWLEDGEMENT

The SSO characterisation work has benefited from useful discussions with Andrew Brown.

7. REFERENCES

Gregory, D., G.J. Shutts and J.R. Mitchell, 1998: A new gravity wave drag scheme incorporating anisotropic orography and low-level wave breaking: Impact upon the climate of the UK Meteorological Office Unified Model. *Q.J.R.Meteorol.Soc.*, **124**, 463–493

Palmer, T.N., Shutts, G.J. and Swinbank, R., 1986. Alleviation of a systematic westerly bias in general circulation and numerical weather prediction models through an orographic gravity wave drag parametrization. *Q. J. R. Meteorol. Soc.*,**112**,1001–1039

Taylor, P.A., Gong, W., Mengesha, Y., Weng, W., Xu, D. and Zhou, J., 1997. "Boundary-layer modelling of neutral and stably-stratified flow over hills, with emphasis on the drag" in proceedings of ECMWF seminar, 10-12 November 1997, on Orography. Available from the European Centre for Medium-Range weather forecasts, Shinfield Park, Reading, Berkshire, RG2 9AU.

Uhrner, U. 2001. The impact of new subgrid scale orography fields on the ECMWF

model. ECMWF Technical Memorandum No. 329. Available from the European Centre for Medium-Range weather forecasts, Shinfield Park, Reading, Berkshire, RG2 9AU.

Webster, S., Brown, A.R., Cameron, D.R. and Jones, C.P., 2003. Improvements to the Representation of Orography in the Met Office Unified Model. *Q. J. R. Meteorol. Soc.*,**129**,1989–2010.